First Draft
December 20, 2011

2D–4D Correspondence: Towers of Kinks Versus Towers of Monopoles in $\mathcal{N} = 2$ Theories

Pavel A. Bolokhov [a,b], **Mikhail Shifman** [a] **and Alexei Yung** [a,c]

[a] *William I. Fine Theoretical Physics Institute, University of Minnesota, Minneapolis, MN 55455, USA*

[b] *Theoretical Physics Department, St.Petersburg State University, Ulyanovskaya 1, Peterhof, St.Petersburg, 198504, Russia*

[c] *Petersburg Nuclear Physics Institute, Gatchina, St. Petersburg 188300, Russia*

Abstract

We continue to study the BPS spectrum of the $\mathcal{N} = (2,2)$ CP^{N-1} model with the $\mathcal{Z}_N$-symmetric twisted mass terms, with emphasis on semiclassical analysis at large masses. "Extra" states found previously [1] are shown to be bound states of topologically-charges kinks and elementary quanta. Quantization of the U(1) kink modulus leads to formation of towers of such states. Our previous consideration was based on the analysis of the central charges, and, thus, presented the necessary conditions for these towers to exist. Dynamical investigation in the quasiclassical limit shows that out of N possible towers only two actually survive in the spectrum for odd N (i.e. only one "extra" tower exist). For even N all would-be "extra" towers do not correspond to actual bound states. Thus, in this case a single tower is present in the spectrum.

For the CP(2) model the curves of the marginal stability (CMS) are discussed in detail. We also comment on 2D–4D correspondence. In this point we overlap and completely agree with Dory and Petunin.

Contents

1 Introduction

The observation of the exact nonperturbative coincidence between the BPS spectrum of the kinks in the two-dimensional CP($N-1$) models with twisted masses and the BPS spectrum of the monopole-dyons in the four-dimensional Seiberg–Witten solution [2] dates back to 1998 [3]. On the four dimensional side this coincidence is for a particular vacuum of $\mathcal{N}=2$ supersymmetric QCD with gauge group U(N) in which a maximal number $r=N$ of quark flavors condense. This observation was understood and interpreted in clear-cut physical terms after the discovery of non-Abelian strings [4, 5] in the $r=N$ Higgs vacuum of $\mathcal{N}=2$ Yang–Mills and the discovery of confined monopoles attached to them [6, 7] (represented by kinks in the effective theory on the string world sheet). It is crucial that the monopole-dyon mass on the Coulomb branch of super QCD in the $r=N$ vacuum is given by the same formula as the mass in the presence of the Fayet-Iliopoulos term. The underlying reason was explained in [6]. The above results set the stage for the development of the 2D–4D correspondence in this particular problem.

An immediate consequence of the spectral coincidence in two and four dimensions (in the Bogomol'nyi–Prasad–Sommerfield [8], BPS for short, sectors) is the coincidence of the curves of marginal stability (CMS) or the domain wall crossings. These curves, being established in two dimensions for kinks can be immediately elevated to four dimensions, for monopole-dyons. Generally speaking, for non-Abelian strings in SU(N) gauge theories there are N appropriate mass parameters. Correspondingly, there are N twisted mass parameters in the two-dimensional CP($N-1$) models (considered in the gauge formulation). Each mass parameter is a complex number. Therefore, in the general case one has to deal with highly multidimensional wall crossings.

In [9] it was pointed out that extremely beneficial for various physical applications was a special choice

$$m_k \;=\; m_0\cdot e^{2\pi i k/N}\,, \qquad\qquad k\;=\;0\,,\;1\,,\;\ldots\,,\;N-1\,; \tag{1.1}$$

preserving a discrete Z_N symmetry of the model. Then there is only one adjustable mass parameter m_0, and the wall crossings reduce to a number of CMS on the complex plane of m_0. We will refer to (1.1) as the Z_N symmetric masses.

These CMS were studied several times in the past. For CP(1) the result was found in [10]. In this case the solution is clear and simple; no questions as to its

validity arise. A more contrived case of CP($N-1$) (with $N \geq 3$) was addressed in [11, 1]. A detailed study carried out in [1] revealed the existence of a richer kink spectrum than was originally anticipated [3]. In particular, the existence of $(N-1)$ towers was argued replacing a single tower discussed in [3]. However, shortly after, we realized that we had analyzed only necessary conditions for these towers to exist, leaving the sufficient conditions aside. In this paper we close this gap. We find that, although (based on the analyses of the central charges) $(N-1)$ towers could exist, in fact, the sufficient conditions are met only for two towers for odd N and a single tower for even N. A generic form of the sufficient conditions were discussed long ago [17]. The second tower for odd N appears as a collection of bound states of the appropriate kinks with a quantum of an elementary excitation carrying no topological number. In four-dimensional language this is a bound (s)quark/gauge boson.

On the four-dimensional side the general theory of the wall crossing was worked out in [12]. Its consequences for the monopole-dyons in the case of the Z_N symmetric masses (1.1) are studied [1] in [13]. Our task is to analyze the kink spectrum and the corresponding CMS in two dimensions, taking account of the sufficient conditions mentioned above, and compare the result with that in four dimensions, thus demonstrating the power of 2D–4D correspondence.

Our strategy will be as follows. We will focus on the first nontrivial case, namely CP(2) model, in which we will carry out a complete quasiclassical analysis of the kink (dyon) bound states with elementary excitation quanta at large masses. We then determine all relevant curves of marginal stability and explain the survival of three Hori–Vafa [14] states in the physical spectrum at small (or vanishing) twisted masses. Then we will generalize the lessons obtained in CP(2) to higher values of N.

2 Prerequisites

In our previous paper [1] for the sake of defining the spectrum we introduced a function $U_0(m_0)$,

$$U_0(m_0) \;=\; \left(e^{2\pi i/N} \;-\; 1\right)\cdot \mathcal{W}(\sigma_0)\,, \tag{2.1}$$

which we argued to be a single-valued quantity in a physical region of the mass parameter m_0, The $\mathcal{Z}_N$ invariance divides the complex plane of m_0 into N physically

[1] We are grateful to the authors for providing us with a draft of their paper prior to its publication.

equivalent sectors, each having the angle $2\pi/N$. Each sector covers the entire complex plane of m_0^N. It follows, say, from the θ dependence that m_0^N is the appropriate physical parameter.

We demonstrated that the mirror-symmetry analysis requires N states to exist at strong coupling, with the central charges

$$\mathcal{Z} \;=\; U_0(m_0) \;+\; i\, m_k\,. \tag{2.2}$$

We argued that continuations of these states to weak coupling should be promoted to "towers" corresponding to nonminimal values of the U(1) kink modulus. The question remained open at that time was as follows: "whether or not these states represent actual bound states in the physical spectrum, and – if yes – what are their dynamical components?"

Before turning to these questions, let us first show how the moduli space of the parameter m_0 looks in the CP^{N-1} models, and, in particular, CP^2 (i.e. $N = 3$). Such an analysis is also helpful in view of the related question of 2D–4D correspondence which will be addressed later.

It turns out that $U_0(m_0)$ by itself does not provide a meaningful topological contribution to the central charge. Speaking in terms of four dimensions, one would like to be able to single out the magnetic contribution $\vec{n}_m \cdot \vec{a}_D$ in the central charge. We argue below that $U_0(m_0)$ by itself does not completely account for the magnetic/topological part. Jumping ahead of ourselves, we can state that, depending on the patch on the moduli space, the topological part is given by

$$U_0 \;+\; i\, m_k \;=\; \mathcal{W}(\sigma_1) \;-\; \mathcal{W}(\sigma_0)\,, \qquad\qquad k \;=\; 0,\, ...\,,\, N-1\,. \tag{2.3}$$

All these quantities are functions of our single free parameter, m_0. A reference patch can be defined in such a way that the topological part reduces to

$$U_0 \;+\; i\, m_s \;=\; \mathcal{W}(\sigma_1) \;-\; \mathcal{W}(\sigma_0)\,. \tag{2.4}$$

Here s is $0\,,\; 1\,,\; ...\,,\; N-1$ and is chosen once and globally. It is this contribution that one needs to identify with $\vec{n}_m \cdot \vec{a}_D$. The strong coupling spectrum (2.2) can then be written as

$$\mathcal{W}(\sigma_1) \;-\; \mathcal{W}(\sigma_0) \;+\; i\,(m_k \,-\, m_s)\,. \tag{2.5}$$

In this form, the central charges are very suggestive to be those corresponding to the bound states of a kink and elementary quanta [17]. Of course, it is not apriori

clear which of three states appearing in (2.5) is the lightest (i.e. the kink per se), and which is the bound state. This has to be established by a direct examination.

As indicated above, in four dimensions the lightest kink will correspond to the monopole. Then there are two higher states: the dyon and the bound state of a monopole and a quark. Before discussing the semiclassical implications of such an interpretation, we first consider the moduli space of the mass parameter, in order to correctly introduce the above quantities.

3 Exact Analysis

In the $\mathcal{N} = 2$ supersymmetric CP^{N-1} theory one has the exact superpotential which describes the entire BPS spectrum nonperturbatively. We adopt a normalization, in which the vacuum values of the exact superpotential take the form

$$\mathcal{W}(\sigma_p) \;\; = \;\; -\,\frac{1}{2\pi}\Big\{\, N\,\sigma_p \;+\; \sum_j m_j\,\ln\,\frac{\sigma_p - m_j}{\Lambda}\,\Big\}\,. \tag{3.1}$$

Here and in the remainder of this paper we put the (nonperturbative) dynamical scale parameter Λ to one. Moreover, σ_p is the position of the p-th vacuum. In our case of the $\mathcal{Z}_N$-symmetric twisted masses, the vacua lie at

$$\sigma_p^N \;\; = \;\; 1 \;\; + \;\; m_0^N\,. \tag{3.2}$$

All these quantities become functions of a single parameter m_0. The spectrum, *i.e.* the central charges of both perturbative and nonperturbative states, are given by the differences of the vacuum values of the superpotential. The masses of the elementary BPS kinks will be given by the differences of the superpotential in two neighbouring vacua.. Because of the $\mathcal{Z}_N$ symmetry of the problem one can always choose them latter to be the 0-th and the first vacua, i.e. $p = 0, 1$. The masses of the elementary states (i.e. without topological charges) are obtained as differences of the superpotential in the same vacua, but with the mass parameter m_0 sitting on different branches of the relevant logarithms.

The problem with these expressions, as emphasized in [1], is in their multivaluedness. This appears both in the logarithms in Eq. (3.1) as well as in the N-th root in Eq. (3.2). The correct handling of the superpotential involves analysis of the whole complex manifold of the mass parameter. In the case of a general N such a

manifold can have a rather complicated structure. We make a few general statements regarding the superpotential in the CP^{N-1} model, and then pass to building the entire complex manifolds in the cases of CP^1 and CP^2.

3.1 Preliminaries: "smart" and "silly" logarithms

As was pointed out, the expression for $\mathcal{W}(\sigma_0)$ is not unambiguous. Even more so is the expression for the difference

$$\mathcal{W}(\sigma_1) \quad - \quad \mathcal{W}(\sigma_0)\,, \tag{3.3}$$

which describes the physical masses of the BPS states. We need to correctly pin-point what is understood wheone speaks of logarithms and N-th roots in our expressions. We can picture two schemes how one can do this.

We repeat that the entire spectrum is contained in the multivalued expression (3.3). The mass parameter m_0 can travel through different branches of the logarithms, and the latter change as continuous functions. Indeed, the logarithms defined on multiple branches do not have any discontinuities; this is the reason why the branches are introduced in the first place. These are the "smart" logarithms, which are supposed to give us all physical states. They are even slightly "smarter" than ordinary multibranched logarithms, since they also should tell us which states obtained in this way are physically stable and which are not.

Such quantities are difficult to deal with. To handle the multivaluedness, as usual, one introduces branch cuts on a single complex plane. We adopt the following definition of the function $\log\ x$:

$$\log\ x \quad \in \quad \mathcal{R}\,, \qquad\qquad \text{when} \quad x \ > \ 0\,. \tag{3.4}$$

We draw a branch cut of this logarithm to extend from the origin to the negative infinity,

$$\text{branch cut:} \qquad -\infty \quad < \quad x \quad < \quad 0\,, \tag{3.5}$$

and put the argument of complex variable to be in the usual domain,

$$-\pi \quad < \quad \mathrm{Im}\ \log x \quad \leq \quad \pi\,. \tag{3.6}$$

This function is defined on a single complex plane and it does not know about various branches. For this reason such quantities can be called "silly" logarithms. Whenever

x passes to a different branch, one needs to add a $2\pi i$ explicitly. These logarithms have a discontinuity across the branch cut.

To an extent a similar statement applies to the definition of σ_p. However, there is a crucial difference: only a single complex branch of the N-th root corresponds to a physical vacuum. Indeed, at large values of the twisted masses, the vacua σ_p take on their (quasi)classical values,

$$\sigma_p \;\approx\; m_p\,, \qquad\qquad |m_p| \;\gg\; 1\,. \tag{3.7}$$

This can be used for determination of the physical branch of m_0 with respect to σ_p. Stepping out of that branch, leads to the same spectrum obtained with a permutation of the vacua. Although in principle, the analysis of the whole complex manifold should include all physically equivalent branches of the root, we do not do this, limiting ourselves to a single physical branch. Thus, we denote the N-root as a function on a single complex plane,

$$\sqrt[N]{x} \;>\; 0\,, \qquad\qquad \text{when}\;\; x \;>\; 0\,, \tag{3.8}$$

and define

$$\sigma_p \;=\; e^{2\pi i p/N}\cdot\sigma_0 \;=\; e^{2\pi i p/N}\cdot\sqrt[N]{1 \,+\, m_0^N}\,. \tag{3.9}$$

The branch cuts of this root in the m_0 plane should be drawn in such a way as to preserve the classical relation (3.7).

We reiterate that the physical values of the central charge

$$\mathcal{Z} \;=\; \mathcal{W}(\sigma_p) \;-\; \mathcal{W}(\sigma_q) \tag{3.10}$$

are given by the "smart" logarithms in the functions $\mathcal{W}(\sigma)$. In the remainder of the paper, however, we will define the superpotential $\mathcal{W}(\sigma_p)$

$$\mathcal{W}(\sigma_p) \;=\; -\,\frac{1}{2\pi}\Big\{\,N\,\sigma_p \,+\, \sum_j m_j\,\log\,\big(\sigma_p - m_j\big)\,\Big\} \tag{3.11}$$

as a function of "silly" logarithms. For each moduli manifold, we therefore will need to introduce a set of branch cuts and specify how the logarithms should jump in order to account for passing onto a different branch. Each such jump, proportional to the mass m_j, should imitate the "smart" logarithm, which is continuous. The jump is introduced precisely to compensate for the discontinuity of the "silly" logarithms.

As defined, the function (3.11) does not know which branch we are currently sitting on. Therefore, we will need to also specify a reference point from which we start accounting. All the rest places of the manifold are reached by passing from this reference point along a contour. While passing along the contour, we pick up all the jumps that occur on the "edges" of branches, while, again, (3.11) does not know that we are in fact jumping from branch to branch.

3.2 Complex manifold of m in CP^{N-1}

The complex manifold for a general CP^{N-1} case will be rather complicated and include multiple branch cuts of the logarithms. We do not perform a full analysis of all such manifolds, which will also depend on the parity of N. But we still make a few general statements regarding these manifolds and the behaviour of function $\mathcal{W}(\sigma_p)$. For simplicity, we denote it as

$$\mathcal{W}_p \quad \stackrel{\text{def}}{=} \quad \mathcal{W}(\sigma_p)\,, \tag{3.12}$$

and always remember that it is a function of m_0.

Figure 1 shows a schematic appearance of a moduli space in CP^{N-1}. The complex plane is diced by various branch cuts of the logarithms. We immediately comment that these branch cuts are non-compact, *i.e.* they extend from infinity to infinity. This is related to the fact that the logarithms depend on combinations $\sigma_p - m_j$, rather than just on masses m_j themselves. Branch cuts appear in the places where these differences become real and negative. As such differences never vanish for finite m_0, the branch cuts may terminate only at infinity. In general, each branch cut is shared by multiple logarithms.

There are N AD points which are located at positions

$$m_0^{\mathrm{AD}}\,: \qquad \left(m^{\mathrm{AD}}\right)^N \quad = \quad -1\,. \tag{3.13}$$

The reason for the particular numbering of the AD points shown in the figure will become clear in just a moment. The points are enclosed by "cups" of hyperbolic-shaped logarithmic branch cuts. There are also $N-1$ branch cuts of the N-root coming from the definition of σ_p (3.2). They can be chosen so as to connect the AD points, as shown by the dashed lines. As one crosses such a branch cut, the phase of each σ_p experiences a jump, coherent to classical relation (3.7). If one starts at

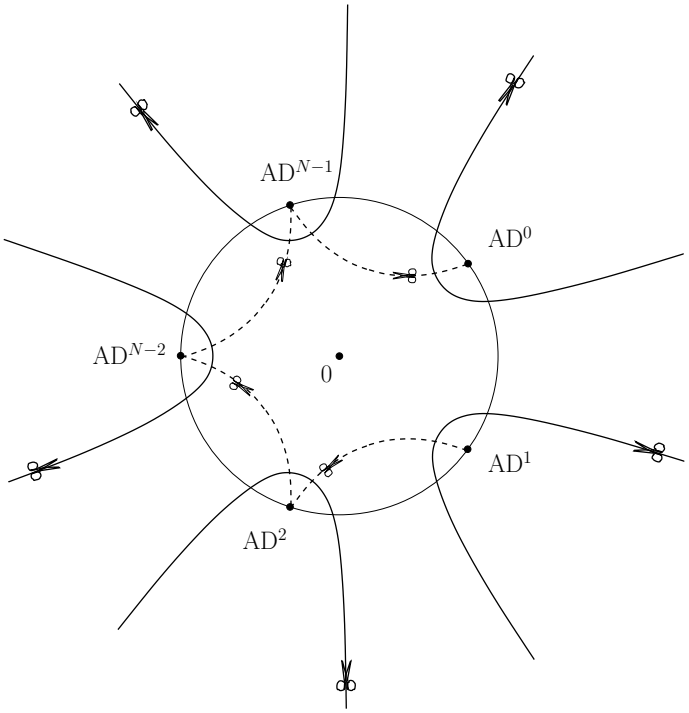

Figure 1: General appearance of a complex moduli space of m in the case of CP^{N-1}. Solid lines sketch the logarithmic branch cuts, dashed lines show the branch cuts of the N-root in σ. See text.

Figure 2: Stretched branch cuts of σ in CP^{N-1}.

the origin and crosses the branch cut connecting AD^{N-1} and AD^0, the vacua shift as $\sigma_p \to \sigma_{p-1}$. If one instead crosses the branch cut connecting AD^{N-2} and AD^{N-1}, the shift will be $\sigma_p \to \sigma_{p-2}$. Following further counter-clockwise, if one crosses the k-th branch cut that connects AD^{N-k} to AD^{N-k+1} when passing from the inside outside, the vacua shift by k turns

$$\sigma_p \quad \to \quad \sigma_{p-k}\,. \tag{3.14}$$

In accord with this, a branch cut of logarithm $\log(\sigma_p - m_j)$ turns into a branch cut of $\log(\sigma_{p\pm k} - m_j)$ after it crosses the k-th branch cut of σ. The plus or minus sign will of course depend on the direction of this crossing. The branch cut of $\log(\sigma_p - m_j)$ itself comes off the physical plane.

For what follows, it is convenient to deform the branch cuts of σ so that they almost touch the origin. Each cut will start from an AD point, come infinitesimally close to the origin in a straight line, then turn around and follow to the other AD point also in a straight line, this way making a letter "v". The system of the σ branch cuts will then form a star with the centre at the origin, as sketched in Fig. 2. The convenience of such a configuration of cuts now shows in a simple relation,

$$\text{as} \quad m_0 \quad \to \quad e^{2\pi i/N}\, m_0\,, \qquad\qquad \sigma_p \quad \to \quad e^{2\pi i/N}\sigma_p\,. \tag{3.15}$$

That is, as m_0 jumps from one "sector" to another, the phase of σ_p jumps accordingly. That this is so at the weak coupling $|m_0| \gg 1$ is not a surprise, but a consequence of Eq. (3.7). In the region of small m_0, however, this did not have to be so, and we have had to arrange the branch cuts in a special way so that relation (3.15) is retained.

Besides introducing the branch cuts, we also need to specify a reference point from which we start counting the central charge. We notice that, any AD point would do in particular. Say we pick $\mathrm{AD}^{(p)}$. Then we automatically define the central charge of an elementary kink to vanish at $\mathrm{AD}^{(p)}$, just because all σ's are equal at an AD point. The value of the central charge in other places, in particular at other AD points, is obtained by following a path connecting the reference point and the

destination point, and accounting for the branch cuts along the way. The central charge of a kink will not vanish at other AD points.

Since our problem has a Z_N symmetry, the complex plane of m_0 is split into N equivalent physical regions. Each physical region contains exactly one AD point. It does not matter where to start measuring the regions from. Because of the different branch cuts, the regions might seem non-equivalent to each other. The equivalence is of course reflected in the coincidence of the physical spectra in all these regions.

The description of the complex space given above is enough for us to introduce two relations which have direct connection to $\mathcal{Z}_N$ symmetry of the theory. We notice that the superpotential

$$\mathcal{W}_p \;\; = \;\; - \; \frac{1}{2\pi} \Big\{ N \, \sigma_p \; + \; \sum_j \, m_j \, \ln \, \big(\sigma_p - m_j \big) \Big\} \tag{3.16}$$

seemingly has a $\mathcal{Z}_N$ symmetry of its vacuum values. Is it true indeed that the vacuum values of $\mathcal{W}$ sit on a circle? The answer is no. Instead, the differences of the vacuum values do,

$$\mathcal{W}_{p+2} \;\; - \;\; \mathcal{W}_{p+1} \;\; = \;\; e^{2\pi i/N} \Big(\mathcal{W}_{p+1} \;\; - \;\; \mathcal{W}_p \Big) \, . \tag{3.17}$$

Similar relations for the vacuum values themselves depend on the location in the moduli space. For us, immediate vicinities of the AD points are important reference locations. The branch cuts of the logarithms form "cups" around each of the AD points. Inside each of the cup, the following relations can be inferred,

$$\mathcal{W}_{p+1} \;\; = \;\; e^{2\pi i/N} \cdot \mathcal{W}_p \;\; + \;\; i \, m_s \, , \tag{3.18}$$

and

$$\mathcal{W}_p \, (e^{2\pi i/N} \cdot m_0) \;\; = \;\; e^{2\pi i/N} \cdot \mathcal{W}_p \, (m_0) \;\; + \;\; i \, m_s \, . \tag{3.19}$$

Here $s = 0$ for $\mathrm{AD}^{(0)}$, $s = 1$ for $\mathrm{AD}^{(1)}$ *etc*, gives the numeration to AD points as shown in Fig. 1.

As an application, Eq. (3.18) immediately gives us the values of $\mathcal{W}_p$ at AD points. Indeed, at any such point $\sigma_p = 0$ and so all $\mathcal{W}_p$ are equal. Therefore,

$$\big(\, e^{2\pi i/N} \;\; - \;\; 1 \, \big) \; \mathcal{W}_p \Big|_{\mathrm{AD}^{(s)}} \;\; = \;\; - \; i \, m_s \, . \tag{3.20}$$

The right hand side is different for all AD points, seemingly. Upon a closer look, the value of m_s at the s-th AD point is independent of s and equals $|m_0| \, e^{i\pi/N}$.

Figure 3: Moduli space of CP^2.

3.3 The moduli space of CP^2

The moduli space in the case of CP^2 is shown in Fig. 3. It has hyperbolic branch cuts of the logarithms, determined by the equations

$$\mathrm{Re}\; m^3 \;=\; -\,\frac{1}{2}\,. \tag{3.21}$$

The branch cuts belonging to the physical plane are marked with subscripts which identify them to their respective logarithms. Each line is a branch cut of two different logarithms. The branch cuts of σ, as discussed previously, can be chosen to connect the AD points. As the logarithm lines cross the σ branch cuts, they turn into branch cuts of other logarithms, in accord with (3.14).

As discussed earlier, the logarithmic cuts form cups around the AD points. Inside these cups, the following relations hold for the vacuum values of the superpotential,

$$\mathcal{W}_{p+1} \;=\; e^{2\pi i/3}\cdot\mathcal{W}_p \;+\; i\,m_s\,, \qquad s\;=\;0,\;1,\;2\,. \tag{3.22}$$

and

$$\mathcal{W}_p\,(e^{2\pi i/3}\cdot m_0) \;=\; e^{2\pi i/3}\cdot\mathcal{W}_p\,(m_0) \;+\; i\,m_s \qquad s\;=\;0,\;1,\;2\,. \tag{3.23}$$

Everywhere *outside* these cups, the superpotential values *are* sitting on the circle,

$$\mathcal{W}_{p+1} \;=\; e^{2\pi i/3}\cdot\mathcal{W}_p \qquad \text{(outside the cups)}. \tag{3.24}$$

In particular, this is true on the real positive axis. This circumstance is very helpful in identifying the states seen as kinks in the mirror description.

At this point we do not have yet an exact prescription how to choose a reference point. Let us pick the reference point to be $\mathrm{AD}^{(2)}$,

$$m_{\mathrm{ref}} \;=\; m^{(2)}_{\mathrm{AD}} \;=\; -\,1\,. \tag{3.25}$$

We will justify this choice later. A state with topological charge

$$\vec{T} \;=\; (\,-1\,,\;\;1\,,\;0\,,\;\;\ldots\,,\;\;0\,) \tag{3.26}$$

becomes massless at this point. We shall denote this state with letter $\mathcal{M}$ to symbolize its resemblence with the four-dimensional monopoles. Its central charge is given by

$$\mathcal{Z}_{\mathcal{M}} \;=\; \mathcal{W}_1 \;-\; \mathcal{W}_0\,. \tag{3.27}$$

There are also dyonic states which are known to exist quasiclassically,

$$\vec{T} \;=\; (-1,\;\; 1,\; 0,\;\; \ldots,\;\; 0)\,, \qquad \vec{S} \;=\; (-n,\;\; n,\; 0,\;\; \ldots,\;\; 0)\,, \tag{3.28}$$

where n is an integer, and $\vec{S}$ denotes the set of U(1) charges. The central charges of such states are given by

$$\mathcal{Z}_{\mathcal{D}^{(n)}} \;=\; \mathcal{W}_1 \;-\; \mathcal{W}_0 \;+\; i\,n\,(m_1 \,-\, m_0)\,. \tag{3.29}$$

We denote these dyonic states by $\mathcal{D}^{(n)}$.

There are three physically equivalent regions, each one containing an AD point. The monodromies of the moduli space work in such a way that as one passes from one physical region to the next one counter-clockwise, the difference $\mathcal{W}_1 \,-\, \mathcal{W}_0$ gains one unit of the U(1) charge,

$$\mathcal{W}_1 \;-\; \mathcal{W}_0 \quad\to\quad \mathcal{W}_1 \;-\; \mathcal{W}_0 \;+\; i\,(m_1 \,-\, m_0)\,. \tag{3.30}$$

Since the $\mathcal{M}$ state becomes massless at $\mathrm{AD}^{(2)}$, the state $\mathcal{D}^{(1)}$ will become massless at $\mathrm{AD}^{(0)}$, and the state $\mathcal{D}^{(-1)}$ at $\mathrm{AD}^{(1)}$. The paths connecting the initial point $\mathrm{AD}^{(2)}$ and the destination points $\mathrm{AD}^{(0)}$ and $\mathrm{AD}^{(1)}$ lie outside the unit circle region, and extend clockwise and counter-clockwise correspondingly. If we further extend these paths through their AD points and into the circle towards the origin, the masses of the states will become

$$\mathcal{W}_1 \;-\; \mathcal{W}_0 \;+\; i\,m_{0,1}\,. \tag{3.31}$$

Now if take the $\mathcal{M}$ state and push it through the point $\mathrm{AD}^{(2)}$ towards the origin, its mass will become $\mathcal{W}_1 \,-\, \mathcal{W}_0 \,+\, i\,m_2$, again, because of the branch cuts. All three states therefore can be written as

$$\mathcal{W}_1 \;-\; \mathcal{W}_0 \;+\; i\,m_k\,, \qquad\qquad k \;=\; 0,\; 1,\; 2\,. \tag{3.32}$$

Since in the area near the origin $\mathcal{W}_1 \;=\; e^{2\pi i/3}\,\mathcal{W}_0$, we obtain all three states predicted by the mirror theory,

$$(e^{2\pi i/3} \;-\; 1)\,\mathcal{W}_0 \;+\; i\,m_k\,, \qquad\qquad k \;=\; 0,\; 1,\; 2\,. \tag{3.33}$$

To clarify, these states are not the original dyonic states $\mathcal{D}^{(n)}$ with $n = -1, 0$ and 1. They would be such if we had followed one and the same path for all three states from $\mathrm{AD}^{(2)}$ to the origin, while we followed different paths. The procedure that we have done shows how the monodromies can be used to construct the spectrum seen in the mirror representation.

We are now allowed to proceed with the three states into the quasiclassical region. The simplest way to do this is to follow the real positive axis from the origin towards infinity. As it will turn out, the quantum numbers of the three states that we have identified correspond to those of a purely topological state, a dyonic state, and a bound state of a topological and elementary states. The existence of the first two in the quasiclassical region $m \gg 1$ does not pose a doubt. Below we review the quasiclassical picture exhibiting the existence of the bound states at weak coupling.

4 Quasiclassics

Strong-coupling analysis by means of mirror symmetry predicts that in the neighbourhood of the origin there are N states. What remains of them at weak coupling, can they be seen quasiclassically? In this section we review the problem of finding the corresponding states at weak coupling, and reconfirm the result of [3]. In the case of $\mathcal{Z}_N$ symmetric masses the result proves the existence of one bound state of a kink and an elementary quantum ψ_k with $k = (N+1)/2$ in the case when N is odd. Quantization of the U(1) coordinate of the kink then raises a tower of bound states of dyonic kinks and the elementary quantum. Importantly, only the "strong-coupling bound state" is seen in quasiclassics. There are no bound states at weak coupling when N is even.

4.1 The central charge

The classical expression for the central charge has two contributions [10]: the Noether and the topological terms,

$$\mathcal{Z} \;=\; i\, M_a\, q^a \;+\; \int dz\, \partial_z\, O\,, \qquad\qquad a \;=\; 1,\, ...\, N-1\,. \tag{4.1}$$

where M_a are the twisted masses (in the geometric formulation),

$$M_a \;=\; m_a \;-\; m_0\,, \tag{4.2}$$

m^a ($a = 1,\ 2,\ ...,\ N$) are the masses in the gauge formulation, and the operator O consists of two parts, canonical and anomalous,

$$O \;=\; O_{\rm canon} + O_{\rm anom}, \tag{4.3}$$

$$O_{\rm canon} \;=\; \sum_{a=1}^{N-1} M_a D^a, \tag{4.4}$$

$$O_{\rm anom} \;=\; -\frac{N\, g_0^2}{4\pi}\, \left(\sum_{a=1}^{N-1} M_a D^a + g_{i\bar{j}}\, \bar{\psi}^{\bar{j}}\, \frac{1-\gamma_5}{2}\, \psi^i \right). \tag{4.5}$$

Moreover, the Noether charges q^a can be obtained from $N-1$ U(1) currents J^a_μ defined as [2]

$$\begin{aligned} J^a_{RL} &= g_{i\bar{\jmath}}\,\overline{\phi}^{\bar{\jmath}}\,(T^a)^{i\bar{\jmath}}\,i\overleftrightarrow{\partial}_{RL}\,\phi^i \\ &+ \frac{1}{2}\,g_{i\bar{\jmath}}\,\overline{\psi}^{\bar{m}}_{LR}\,\left((T^a)_{\bar{m}}{}^{\bar{p}}\,\delta_{\bar{p}}{}^{\bar{\jmath}} + \overline{\phi}^{\bar{r}}\,(T^a)_{\bar{r}}{}^{\bar{k}}\,\Gamma^{\bar{\jmath}}_{\bar{k}\bar{m}}\right)\,\psi^i_{LR} \\ &+ \frac{1}{2}\,g_{i\bar{\jmath}}\,\overline{\psi}^{\bar{\jmath}}_{LR}\,\left(\delta^i{}_p\,(T^a)^p{}_m + \Gamma^i_{mk}\,(T^a)^k{}_r\,\phi^r\right)\,\psi^m_{LR} \end{aligned} \tag{4.6}$$

in the geometric representation, and

$$\begin{aligned} J^a_{RL} &= i\,\overline{n}_a\overleftrightarrow{\partial}_{RL}n^a - |n^a|^2\cdot i\,(\overline{n}\overleftrightarrow{\partial}\,n) \\ &+ \overline{\xi}^a_{LR}\,\xi^a_{LR} - |n^a|^2\cdot(\overline{\xi}_{LR}\,\xi_{LR}) \end{aligned} \tag{4.7}$$

in the gauged formulation. Here

$$(T^a)^i_k = \delta^i_a\delta^a_k\,, \quad \text{(no summation over } a!) \tag{4.8}$$

and a similar expression for the overbarred indices. Finally, D^a are the Killing potentials,

$$D^a = r_0\,\frac{\overline{\phi}\,T^a\,\phi}{1+|\phi|^2} = r_0\,\frac{\overline{\phi}^a\,\phi^a}{1+|\phi|^2}\,. \tag{4.9}$$

The generators T^a always pick up the a-th component. In this expression,

$$r_0 = \frac{2}{g_0^2} \tag{4.10}$$

is a popular alternative notation for the sigma model coupling.

Note that Eq. (4.9) contains the bare coupling. It is clear that the one-loop correction must (and will) convert the bare coupling into the renormalized coupling. The anomalous part $O_{\rm anom}$ is obtained at one loop. Therefore, in the one-loop approximation for the central charge it is sufficient to treat $O_{\rm anom}$ in the lowest order. Moreover, the bifermion term in $O_{\rm anom}$ plays a role only in the two-loop approximation. As a result, to calculate the central charge at one loop it is sufficient to analyze the one-loop correction to $O_{\rm canon}$. The latter is determined by the tadpole graphs in Fig 4. As usual, the simplest way to perform the calculation is the background

[2] There is a typo in the definition of these currents in [10].

Figure 4: Tadpoles contributing to the topological term O.

field method. The part of the central charge under consideration is determined by the value of the fields at the spatial infinities. In the CP^2 model to be considered below there are three vacua and three possible ways of interpolation between them. All kinks are equivalent. of the soliton interpolating between vacua (0) and (1)

$$\phi^1(z) \;=\; e^{|M^1|z}\,, \qquad\qquad \phi^2(z) \;=\; \phi^3(z) \;=\; ... \;=\; 0\,. \tag{4.11}$$

That this is the right kink can be seen in the gauged formulation,

$$\begin{aligned} n^0 &= \frac{1}{\sqrt{1\;+\;e^{2|M^1|z}}}\,, \\ n^1 &= \frac{e^{|M^1|z}}{\sqrt{1\;+\;e^{2|M^1|z}}}\,, \\ n^2 &= 0\,, \\ &\vdots \\ n^k &= 0\,, \\ &\vdots \\ n^{N-1} &= 0\,. \end{aligned} \tag{4.12}$$

In this background, D^a taken at the edges of the worldsheet yields just the coupling constant:

$$D^a\Big|_{-\infty}^{+\infty} \;=\; r\,. \tag{4.13}$$

We will see that the one-loop corrected contribution to the central charge of the kink is

$$\mathcal{Z} \;\supset\; \frac{N}{2\pi}\,M^1\,\ln\frac{|M^a|}{\Lambda}\,. \tag{4.14}$$

As for the Noether contribution, the quantization of the "angle" coordinate of the kink gives

$$i\,n\,M^1\,, \tag{4.15}$$

Figure 5: Mass parameters M_1 and M_2 figuring in the geometric formulation of CP^2.

with $q^1 = n$ an integer number. As for the other q^k, the kink does not have fermionic zero-modes of ψ^k with $k = 2, 3, \ldots N-1$. However, we will argue that in the case of odd N there is a *non*-zero mode relevant to the problem of multiple towers that we consider (in fact, the existence of this nonzero mode was noted by Dorey *et al.* [17]). This mode describes a bound state of the kink and a fermion ψ^k for $k = (N+1)/2$.

4.2 Semiclassical calculation of the central charge in $\mathbf{CP^2}$

If the twisted masses M_a satisfy the condition

$$|M_a| \gg \Lambda\,, \tag{4.16}$$

then we find ourselves at weak coupling where the one-loop calculation of the central charges will be sufficient for our purposes. This calculation can be carried out in a straightforward manner for all CP^{N-1} models, but for the sake if simplicity we will limit ourselves to CP^2. Generalization to larger N is quite obvious.

In CP^2 there are two twisted mass parameters, M_1 and M_2, as shown in Fig. 5. Accordingly, there are two U(1) charges, see Eq. (4.6). The Noether charges are not renormalized; therefore we will focus on the topological part represented by the Killing potentials, which are renormalized.

4.2.1 Topological contribution

One-loop calculations are most easily performed using the background field method. For what follows it is important that $\phi_{\mathrm{b}}^2 \equiv 0$ for the kink under consideration. If so, all off-diagonal elements of the metric $g_{i\bar{j}}$ vanish, while the diagonal elements take the form

$$\begin{aligned} g^{\mathrm{b}}_{1\bar{1}} &\equiv g_{1\bar{1}}\Big|_{\phi_{\mathrm{b}}} = \frac{2}{g_0^2}\,\frac{1}{\chi^2}\,, \\ g^{\mathrm{b}}_{2\bar{2}} &\equiv g_{2\bar{2}}\Big|_{\phi_{\mathrm{b}}} = \frac{2}{g_0^2}\,\frac{1}{\chi}\,, \end{aligned} \tag{4.17}$$

where

$$\chi = 1 + \left|\phi^1_{\rm b}\right|^2 \tag{4.18}$$

At the boundaries $\phi^{1,2}_{\rm b}$ take their (vacuum) coordinate-independent values; therefore, the Lagrangian for the quantum fields can be written as

$$\mathcal{L} = g^{\rm b}_{1\bar{1}} \left|\partial^\mu \phi^1_{\rm qu}\right|^2 + g^{\rm b}_{2\bar{2}} \left|\partial^\mu \phi^2_{\rm qu}\right|^2 + ... \tag{4.19}$$

where the ellipses stand for the terms irrelevant for our calculation.

The Killing potentials can be expanded in the same way. Under the condition $\phi^2_{\rm b} \equiv 0$ we arrive at

$$\begin{aligned} D^1 &= D^1\Big|_{\phi_{\rm b}} + \frac{2}{g_0^2}\,\frac{1-\left|\phi^1_{\rm b}\right|^2}{\chi^3}\,\left|\phi^1_{\rm qu}\right|^2 - \frac{2}{g_0^2}\,\frac{\left|\phi^1_{\rm b}\right|^2}{\chi^2}\,\left|\phi^2_{\rm qu}\right|^2 + ...\,, \\ D^2 &= 0\,. \end{aligned} \tag{4.20}$$

Equation (4.19) implies that the Green's functions of the quantum fields are

$$\left\langle \phi^1_{\rm qu}, \phi^1_{\rm qu} \right\rangle = \frac{g_0^2\,\chi^2}{2}\,\frac{i}{k^2 - \left|M\right|^2}\,, \qquad \left\langle \phi^2_{\rm qu}, \phi^2_{\rm qu} \right\rangle = \frac{g_0^2\,\chi}{2}\,\frac{i}{k^2 - \left|M\right|^2}\,. \tag{4.21}$$

where

$$|M| \equiv |M_1| \equiv |M_2|\ . \tag{4.22}$$

Now, combining (4.20) and (4.21) to evaluate the tadpoles graphs of Fig. XXX with $\phi^1_{\rm qu}$ and $\phi^2_{\rm qu}$ running inside we arrive at

$$\begin{aligned} D^1_{\rm one-loop} &= \frac{1}{4\pi}\,\ln\frac{\left|M_{\rm uv}\right|^2}{\left|M\right|^2} \\ &\times \left(\frac{1-\left|\phi^1_{\rm b}\right|^2}{\chi} - \frac{\left|\phi^1_{\rm b}\right|^2}{\chi}\right)^{\phi^1_{\rm b}=0}_{\phi^1_{\rm b}=\infty} \\ &= \frac{1}{4\pi}\,\ln\frac{\left|M_{\rm uv}\right|^2}{\left|M\right|^2}\,(2+1)\,. \end{aligned} \tag{4.23}$$

where $M_{\rm uv}$ is an ultraviolet cut-off (e.g. the Pauli-Villars regulator mass). The first and second terms in the parentheses come from the $\phi^1_{\rm qu}$ and $\phi^2_{\rm qu}$ loops, respectively. In the general case of the CP^{N-1} model one must replace $2+1$ by $2+1\times(N-2) = N$.

This information allows us to obtain the contribution of the Killing potential to the central charge at one loop, namely,

$$\Delta_{\rm K}\mathcal{Z} = -2M_1\left[\frac{1}{g_0^2} - \frac{3}{4\pi}\left(\ln\left|\frac{M_{\rm uv}}{M}\right| + 1\right)\right] \tag{4.24}$$

Note that the renormalized coupling in the case at hand is [18]

$$\frac{1}{g^2} = \frac{1}{g_0^2} - \frac{3}{4\pi}\ln\left|\frac{M_{\rm uv}}{M}\right| \equiv \frac{3}{4\pi}\ln\left|\frac{M}{\Lambda}\right| . \tag{4.25}$$

For the generic CP^{N-1} model the coefficient 3 in front of the logarithm in (4.25) is replaced by N. Equation (4.25) serves as a (standard) definition of the dynamical scale parameter Λ in perturbation theory in the Pauli-Villars scheme.

4.2.2 Contribution coming from the Noether charges

This is not the end of the story, however. We must add to $\Delta_{\rm K}\mathcal{Z}$ a part of the central charge associated with the Noether terms in (4.1), which accounts for the quantization of the fermion zero modes as well as effects of the θ term.

4.2.3 Weak-coupling expansion

We can start from the known superpotential of the Veneziano–Yankielowicz type, and the spectrum that it generates. It gives the exact solution of the CP^{N-1} model with twisted masses in the BPS sector. In our case of $\mathcal{Z}_N$ symmetric twisted masses this superpotential is given in [1].

Here we narrow down to the case of CP^2, with masses that are $\mathcal{Z}_3$ symmetric. The central charge determining the BPS spectrum is given by the difference of the values of the superpotential in two vacua. The general formula adjusted for CP^2 is as follows [1]:

$$\mathcal{Z}\Big|_{-\infty}^{+\infty} \;=\; U_0(m_0) \;+\; i\,n\,M_1 \;+\; i\,m_k \qquad\qquad \text{with } k \;=\; 0,\; 1,\; 2, \tag{4.26}$$

$$\stackrel{|m_0|\to\infty}{\longrightarrow} \frac{3}{2\pi}\,M_1\left\{\ln\frac{|M_1|}{\Lambda_{\rm np}} \;-\; 1 \;-\; \frac{5\,\pi}{6\sqrt{3}}\right\} \;+\; i\,n\,M_1 \;+\; i\,(\,m_k \,-\, m_2\,) \;+\; \ldots$$

where the ellipsis represents suppressed terms dying off as inverse powers of the large mass parameter. Although for our purposes we pick m_0 to be real, expansion (4.26)

is actually valid in the whole sector of

$$-\pi/N \quad < \quad \mathrm{Arg}\, m_0 \quad < \quad +\pi/N\,. \tag{4.27}$$

We have explicitly re-introduced the dynamical scale Λ, which we mark as a "non-perturbative" quantity, as being part of the exact superpotential.

Various contributions are easy to identify in Eq. (4.26). The first term in the figure bracket can be identified with the running coupling constant. The second term comes from the anomaly. The third term is the real addition to the logarithm, and should be absorbed into the dynamical scale Λ. This way, matching with the quasiclassical calculation of the central charge is achieved:

$$\Lambda_{\rm pt} \quad = \quad e^{5\pi/6\sqrt{3}}\,\Lambda_{\rm np}\,. \tag{4.28}$$

4.3 Quasiclassical Kink Solution in CP^2

In this section we will briefly discuss the kink solution in CP^2. In fact, the bosonic part (and its quantization), as well as the fermion zero mode in ψ^1 are the same as in CP^1 [19]. The crucial difference is the occurrence of a localized (but nonzero!) mode in ψ^2.

4.3.1 Kink solution

In the classical kink solution the field ϕ^2 is not involved. The BPS equation for ϕ^1 is the same as in CP^1, namely,

$$\partial_z\phi = |M|\phi\,. \tag{4.1}$$

The solution of this equation can be written as

$$\phi(z) = e^{|M|(z-z_0)-i\alpha}\,. \tag{4.2}$$

Here z_0 is the kink center while α is an arbitrary phase related to $\mathrm{U}(1)_1$. In fact, these two parameters enter only in the combination $|m|z_0 + i\alpha$. The kink center is complexified.

The effect of the modulus α explains the occurrence of $n\,M_1$ from the Noether part.

4.3.2 Quantization of the bosonic moduli

To carry out conventional quasiclassical quantization we, as usual, assume the moduli z_0 and α in Eq. (4.2) to be (weakly) time-dependent, substitute (4.2) in the bosonic part of the Lagrangian, integrate over z and arrive at

$$\mathcal{L}_{\rm QM} = -M_{\rm kink} + \frac{M_{\rm kink}}{2}\dot{z}_0^2 + \left\{ \frac{1}{g^2|M|}\,\dot{\alpha}^2 - \frac{\theta}{2\pi}\,\dot{\alpha} \right\}. \tag{4.3}$$

The first term is the classical kink mass, the second describes free motion of the kink along the z axis. The term in the braces is most interesting. The variable α is compact. Its very existence is related to the exact U(1) symmetry of the model. The energy spectrum corresponding to α dynamics is quantized. It is not difficult to see that

$$E_{[\alpha]} = \frac{g^2|M|}{4}\; q_{\rm U(1)}^2\,, \tag{4.4}$$

where $q_{\rm U(1)}$ is the U(1) charge of the soliton,

$$q_{\rm U(1)} \;\; = \;\; k \;\; + \;\; \frac{\theta}{2\pi}\,, \qquad k \;\in\; \mathcal{Z}\,. \tag{4.5}$$

The kink U(1) charge is no longer integer in the presence of the θ term, it is shifted by $\theta/(2\pi)$.

4.3.3 Fermions in quasiclassical consideration

First we will focus on the zero modes of ψ^1 in the kink background (4.2). The coefficients in front of the fermion zero modes will become (time-dependent) fermion moduli, for which we are going to build corresponding quantum mechanics. There are two such moduli, $\bar{\eta}$ and η.

The equations for the fermion zero modes are

$$\begin{aligned}
\partial_z\psi_L^1 \;\; &-\frac{2}{\chi}\left(\bar{\phi}^1\partial_z\phi^1\right)\psi_L^1 - i\,\frac{1-\bar{\phi}^1\phi^1}{\chi}\,|M|e^{i\beta}\psi_R^1 = 0\,,\\
\partial_z\psi_R^1 \;\; &-\frac{2}{\chi}\left(\bar{\phi}^1\partial_z\phi^1\right)\psi_R^1 + i\,\frac{1-\bar{\phi}^1\phi^1}{\chi}\,|M|e^{-i\beta}\psi_L^1 = 0
\end{aligned} \tag{4.6}$$

(plus similar equations for $\bar{\psi}$; since our operator is Hermitean we do not need to consider them separately.)

It is not difficult to find solution to these equations, either directly, or using supersymmetry. Indeed, if we know the bosonic solution (4.2), its fermionic superpartner — and the fermion zero modes are such superpartners — is obtained from the bosonic one by those two supertransformations which act on $\bar{\phi}$, ϕ nontrivially. In this way we conclude that the functional form of the fermion zero mode must coincide with the functional form of the boson solution (4.2). Concretely,

$$\begin{pmatrix} \psi_R \\ \psi_L \end{pmatrix} = \eta \left(\frac{g^2|M|}{2} \right)^{1/2} \begin{pmatrix} -ie^{-i\beta} \\ 1 \end{pmatrix} e^{|M|(z-z_0)} \tag{4.7}$$

and

$$\begin{pmatrix} \bar{\psi}^1_R \\ \bar{\psi}^1_L \end{pmatrix} = \bar{\eta} \left(\frac{g^2|M|}{2} \right)^{1/2} \begin{pmatrix} ie^{i\beta} \\ 1 \end{pmatrix} e^{|M|(z-z_0)} \,, \tag{4.8}$$

where the numerical factor is introduced to ensure proper normalization of the quantum-mechanical Lagrangian. Another solution which asymptotically, at large z, behaves as $e^{3|M|(z-z_0)}$ must be discarded as non-normalizable.

Now, to perform quasiclassical quantization we follow the standard route: the moduli are assumed to be time-dependent, and we derive quantum mechanics of moduli starting from the original Lagrangian. Substituting the kink solution and the fermion zero modes for Ψ one gets

$$\mathcal{L}'_{\rm QM} = i\,\bar{\eta}\dot{\eta}\,. \tag{4.9}$$

In the Hamiltonian approach the only remnants of the fermion moduli are the anticommutation relations

$$\{\bar{\eta}\eta\} = 1\,, \quad \{\bar{\eta}\bar{\eta}\} = 0\,, \quad \{\eta\eta\} = 0\,, \tag{4.10}$$

which tell us that the wave function is two-component (i.e. the kink supermultiplet is two-dimensional). One can implement Eq. (4.10) by choosing e.g. $\bar{\eta} = \sigma^+$, $\eta = \sigma^-$.

4.3.4 Combining bosonic and fermionic moduli

Quantum dynamics of the kink at hand is summarized by the Hamiltonian

$$H_{\rm QM} = \frac{M_{\rm kink}}{2}\,\dot{\bar{\zeta}}\,\dot{\zeta} \tag{4.11}$$

acting in the space of two-component wave functions. The variable ζ here is a complexified kink center,

$$\zeta = z_0 + \frac{i}{|M|}\,\alpha\,. \tag{4.12}$$

For simplicity, we set the vacuum angle $\theta = 0$ for the time being (it will be reinstated later).

The original field theory we deal with has four conserved supercharges. Two of them, $\mathcal{Q}$ and $\bar{\mathcal{Q}}$, act trivially in the critical kink sector. In moduli quantum mechanics they take the form

$$\mathcal{Q} = \sqrt{M_0}\,\dot{\zeta}\eta\,, \qquad \bar{\mathcal{Q}} = \sqrt{M_0}\,\dot{\bar{\zeta}}\bar{\eta}\,; \tag{4.13}$$

they do indeed vanish provided that the kink is at rest. Superalgebra describing kink quantum mechanics is $\{\bar{\mathcal{Q}}\,\mathcal{Q}\} = 2H_{\rm QM}$. This is nothing but Witten's $\mathcal{N} = 1$ supersymmetric quantum mechanics (two supercharges). The realization we deal with is peculiar and distinct from that of Witten. Indeed, the standard Witten quantum mechanics includes one (real) bosonic degree of freedom and two fermionic, while we have two bosonic degrees of freedom, x_0 and α. Nevertheless, superalgebra remains the same due to the fact that the bosonic coordinate is complexified.

Finally, to conclude this section, let us calculate the U(1) charge of the kink states. Starting from the expression for the $\mathrm{U}(1)_1$ current we substitute the fermion zero modes and get [3]

$$\Delta q_{\mathrm{U}(1)} = \frac{1}{2}[\bar{\eta}\eta] \tag{4.14}$$

(this is to be added to the bosonic part, Eq. (4.5)). Given that $\bar{\eta} = \sigma^+$ and $\eta = \sigma^-$ we arrive at $\Delta q_{\mathrm{U}(1)} = \frac{1}{2}\sigma_3$. This means that the $\mathrm{U}(1)_1$ charges of two kink states in the supermultiplet split from the value given in Eq. (4.5): one has the $\mathrm{U}(1)_1$ charge

$$k + \frac{1}{2} + \frac{\theta}{2\pi}\,,$$

and another

$$k - \frac{1}{2} + \frac{\theta}{2\pi}\,.$$

[3] To set the scale properly, so that the U(1) charge of the vacuum state vanishes, one must antisymmetrize the fermion current, $\overline{\psi}\gamma^\mu\psi \to (1/2)\left(\overline{\psi}\gamma^\mu\psi - \overline{\psi}^c\gamma^\mu\psi^c\right)$ where the superscript c denotes C conjugation.

4.3.5 Bound States of ψ^2

To find the non-zero mode, we write out the linearized Dirac equations in the background of the ϕ^1 kink. For convenience, we rescale the variable z into a dimensionless variable s:

$$s \;=\; 2\,|M^1|\,z\,. \tag{4.15}$$

Then the kink takes the form

$$\phi^1(s) \;=\; e^{s/2}\,, \qquad \text{and} \quad \phi^k(s) \;=\; 0 \qquad \text{for} \;\; k \;>\; 1\,, \tag{4.16}$$

or

$$\begin{aligned} n^0 &= \frac{1}{\sqrt{1\;+\;e^s}}\,, \\ n^1 &= \frac{e^{s/2}}{\sqrt{1\;+\;e^s}}\,, \\ n^2 &= 0\,, \\ &\vdots \\ n^k &= 0\,, \\ &\vdots \\ n^{N-1} &= 0\,. \end{aligned} \tag{4.17}$$

The masses will also turn dimensionless by the same factor,

$$\mu^l \;=\; \frac{m^l}{2|M^1|}\,, \qquad \text{and} \qquad \mu^a_G \;=\; \frac{M^a}{2|M^1|}\,, \tag{4.18}$$

written both for geometric and gauge formulations.

The linearized Dirac equations for the fermion ψ^k with $k \;>\; 1$ then look like

$$\begin{aligned} \left\{\partial_s \;-\; \frac{1}{2}\,f(s)\right\}\,\psi^k_R \;+\; i\,\left(\mu^1_G\,f(s) \;-\; \mu^k_G\right)\cdot\psi^k_L &= i\,\lambda\,\psi^k_L \\ \left\{\partial_s \;-\; \frac{1}{2}\,f(s)\right\}\,\psi^k_L \;-\; i\,\left(\overline{\mu}^1_G\,f(s) \;-\; \overline{\mu}^k_G\right)\cdot\psi^k_R &= -\,i\,\overline{\lambda}\,\psi^k_R\,. \end{aligned} \tag{4.19}$$

Here $f(s)$ is a real function

$$f(s) \;=\; \frac{e^s}{1\;+\;e^s}\,. \tag{4.20}$$

Eigenvalue λ is zero for zero-modes, or gives the energy for non-zero modes. If one starts from the gauged formulation, one arrives at a simpler system, which can be obtained from the above one by redefinition of the functions. That is, the conversion between the geometric and gauge formulations is precisely such as to remove the inhomogeneous term from the figure brackets,

$$\begin{aligned}
\partial_s\,\xi^k_R \;+\; i\,\Big(\mu^1_G\,f(s)\;-\;\mu^k_G\Big)\cdot\xi^k_L \;&=\; i\,\lambda\,\xi^k_L \\
\partial_s\,\xi^k_L \;-\; i\,\Big(\overline{\mu}^1_G\,f(s)\;-\;\overline{\mu}^k_G\Big)\cdot\xi^k_R \;&=\; -\,i\,\overline{\lambda}\,\xi^k_R\,.
\end{aligned} \tag{4.21}$$

This system does not allow normalizable zero modes. However, there is a normalizable non-zero mode with the energy given by the absolute value of

$$\lambda \;=\; -\,\mu^k_G \;+\; \frac{1}{2}\mu^1_G\,. \tag{4.22}$$

The mode is

$$\begin{aligned}
\xi^k_R \;&=\; \left(\frac{e^{\alpha s}}{1\;+\;e^s}\right)^{1/2} \\
\xi^k_L \;&=\; -\,i\,\frac{\overline{\mu}^1_G}{|\mu^1_G|}\cdot\xi^k_R\,.
\end{aligned} \tag{4.23}$$

It is straightforward to show that there exists the corresponding bosonic mode. The relevant part of the Lagrangian is,

$$\mathcal{L} \;=\; g_{i\bar{\jmath}}\,\partial_\mu\phi^i\,\partial^\mu\,\overline{\phi}^{\bar{\jmath}} \;+\; g_{i\bar{\jmath}}\,\mathrm{Re}\,(M^i\,\overline{M}^{\bar{\jmath}})\cdot\phi^i\,\overline{\phi}^{\bar{\jmath}} \;+\; ... \tag{4.24}$$

The corresponding equations of motion are

$$\begin{aligned}
g^{i\bar{k}}\,\frac{\delta\mathcal{L}}{\delta\,\overline{\phi}^{\bar{k}}} \;=\;& -\;\partial^2_\mu\,\phi^i \;-\; \Gamma^i_{pl}\cdot\partial_\mu\phi^p\,\partial^\mu\phi^l \\
&+\;(\,g^{i\bar{k}}\,\partial_{\bar{k}}\,g_{l\bar{\jmath}}\,)\cdot\partial_\mu\phi^l\,\partial^\mu\,\overline{\phi}^{\bar{\jmath}} \;-\; (\,g^{i\bar{k}}\,\partial_{\bar{\jmath}}\,g_{l\bar{k}}\,)\cdot\partial_\mu\phi^l\,\partial^\mu\overline{\phi}^{\bar{\jmath}} \\
&+\;(\,g^{i\bar{k}}\,g_{l\bar{k}}\,)\cdot\mathrm{Re}\,\big(\,M_l\,\overline{M}_{\bar{k}}\,\big)\cdot\phi^l \\
&+\;(\,g^{i\bar{k}}\,\partial_{\bar{k}}\,g_{l\bar{\jmath}}\,)\cdot\mathrm{Re}\,\big(\,M_l\,\overline{M}_{\bar{k}}\,\big)\cdot\phi^l\,\overline{\phi}^{\bar{\jmath}}\,.
\end{aligned} \tag{4.25}$$

Linearization of the equations of motion leads to the equation for the eigenmode ϕ^k:

$$-\partial_s^2\,\phi^k \;+\; f(s)\cdot\partial_s\phi^k \;+\; \left(\left|\mu_G^k\right| \;-\; 2\,\mathrm{Re}\,\left(\mu_G^1\,\overline{\mu}_G^k\right)\,f(s)\right)\,\phi^k \;=\; \lambda\cdot\phi^k\,, \quad (4.26)$$

where $k > 1$. The solution is the same as for the fermionic mode,

$$\phi^k \;=\; \left(\frac{e^{\alpha s}}{1\;+\;e^s}\right)^{1/2}\,, \qquad\qquad \alpha \;=\; \mathrm{Re}\,\frac{M_k}{M_1}\,, \quad (4.27)$$

with the corresponding eigenvalue

$$E^2 \;=\; \left(2\,|M_1|\right)^2\,\lambda \;=\; \left|\,M_k\,\sin\mathrm{Arg}\,\frac{M_k}{M_1}\,\right|^2. \quad (4.28)$$

In this form the eigenmodes are actually correct for CP^{N-1} with arbitrary twisted masses, not necessarily with ones sitting on the circle.

That these modes are BPS can be seen from the expansion of the central charge

$$|\,r\cdot M_1\;+\;i\,M_k\,| \;=\; r\cdot|M_1| \;-\; |M_k|\cdot\sin\mathrm{Arg}\,\frac{M_k}{M_1} \;+\; \ldots\,, \quad (4.29)$$

in the large coupling constant r. This is the central charge of the bound state of a fermion and the kink as discovered by Dorey *et al.* [17], written semi-classically.

The normalizability of the eigenmodes translates into

$$0 \;<\; \mathrm{Re}\,\frac{M_k}{M_1} \;<\; 1\,. \quad (4.30)$$

In the case of $\mathcal{Z}_N$ symmetric masses m_k, this condition is only met for $k = (N+1)/2$ when N is odd, and never met when N is even.

5 Decay Curves

We have explicated that the spectrum at the strong coupling consists of a purely topological state $\mathcal{M}$, a dyonic state $\mathcal{D}$ and a bound state $\mathcal{M}\mathcal{Q}_2$. Here, $\mathcal{Q}_2$ denotes the elementary quantum ψ^2. At weak coupling, aside of $\mathcal{M}$ and $\mathcal{D}$, there is an infinite tower of dyonic kinks $\mathcal{D}^{(n)}$

$$\vec{T} \;=\; (-1,\;\; 1,\;\; 0)\,, \qquad \vec{S} \;=\; (-n,\;\; n,\;\; 0)\,, \tag{5.1}$$

and the bound states $\mathcal{D}^{(n)}\mathcal{Q}_2$ of these dyons with the elementary quanta ψ^2. Plus, there are elementary quanta $\mathcal{Q}_1$ and $\mathcal{Q}_2$.

All these extra states have to decay somewhere on the way from large m to small m. We argue that the primary CMS [1] is responsible for decay of all elementary states and dyonic kinks $\mathcal{D}^{(n)}$. Indeed, the primary CMS is the curve found by the condition of alignment of the central charges of the topological state $\mathcal{M}$ and the first quantum $\mathcal{Q}_1$. If they are aligned with each other, they are also aligned with the central charges of dyons $\mathcal{D}^{(n)}$. Then the quantum $\mathcal{Q}_1$ and the dyons have to decay into the lightest states — the topological state $\mathcal{M}$ and the first dyon $\mathcal{D}^{(1)}$.

The state $\mathcal{Q}_2$ seemingly cannot decay on the primary CMS, since its central charge would not be aligned with any of $\mathcal{M}$ or $\mathcal{D}^{(1)}$. However, there is a different channel of decay, namely, that into the topological states with the charges

$$\vec{T} \;=\; (-1,\;\; 0,\;\; 1)\,. \tag{5.2}$$

Namely, there are completely analogous states $\mathcal{M}'$ and $\mathcal{D}'^{(1)}$ with the above topological charge. We are not considering them, as we have limited ourselves to the discussion of kinks interpolating between the vacua (0) and (1), with the rest of the spectrum recoverable by action of $\mathcal{Z}_3$ symmetry. But the quantum $\mathcal{Q}_2$ is still allowed to decay via any legal mode, and the condition of decaying into $\mathcal{M}'$ and $\mathcal{D}'^{(1)}$ precisely reproduces the condition for the primary CMS.

Finally, the bound states $\mathcal{D}^{(n)}\mathcal{Q}_2$ have two decay modes,

$$\mathcal{D}^{(n)}\mathcal{Q}_2 \;\;\to\;\; \mathcal{D}^{(n)} \;\;+\;\; \mathcal{Q}_2\,, \tag{5.3}$$

and

$$\mathcal{D}^{(n)}\mathcal{Q}_2 \;\;\to\;\; \mathcal{D}^{(n+1)} \;\;+\;\; \mathcal{Q}_{21}\,, \tag{5.4}$$

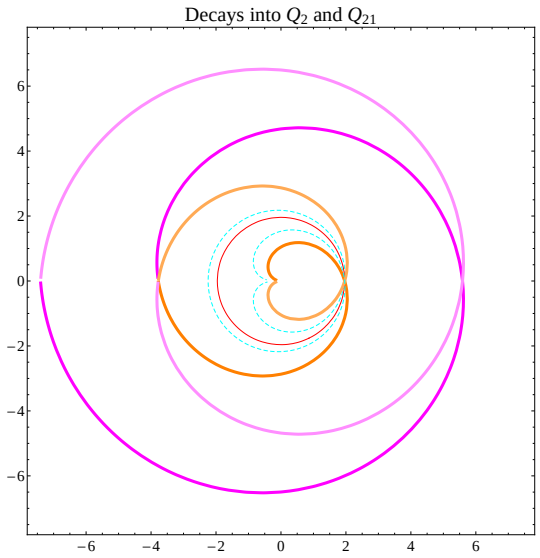

Figure 6: Decay curves in CP^2.

where $\mathcal{Q}_{21}$ has the U(1) charges $\vec{S} = (0, \ -1, \ 1)$ and can be viewed as a bound state of the quantum $\mathcal{Q}_2$ and anti-state $\overline{\mathcal{Q}}_1$.

The corresponding curves are shown in Fig. 6. The decay curves of the bound states represent a spiral that winds outwards. Each next branch of the spiral correspond to the decay of the dyonic state with a greater U(1) number. The above two decay channels induce two symmetric spiral curves.

6 Conclusion

We have re-examined the problem of the spectrum of CP^{N-1} theory with twisted masses. Previous analysis [1] revealed existence of extra states which were not known before. However, the number of towers of such states was found incorrectly. Semiclassical analysis of bound states [3] shows that in a set-up with $\mathcal{Z}_N$ symmetric masses there is only one extra tower of states which was not known to exist, in the case of odd N, and no towers for even N.

In the case of CP^2, the tower does not decay on a single curve, but rather, each bound state of the tower decays on its designated branch of a spiral curve. The elementary states, which correspond to quarks/gauge bosons in four dimensions, decay on the primary CMS. We expect a similar picture to take place for CP^{N-1} with a general odd N. Even more generally, condition (4.30) is not as restricting in a theory with arbitrary distributed twisted masses. Multiple towers of bound states may exist at weak coupling, both for even and odd N. Speaking of wall crossing in terms of decay curves becomes impractical, however.

The correspondence between the spectra of the two-dimensional sigma model and four-dimensional $\mathrm{U}(N)$ QCD in $r = N$ Higgs vacuum elevates this picture into four dimensions. The extra tower of states which exists for odd N correspond to bound states of dyons and quarks.

Acknowledgments

The work of PAB and MS was supported by the DOE grant DE-FG02-94ER40823. The work of AY was supported by FTPI, University of Minnesota, by the RFBR Grant No. 09-02-00457a and by the Russian State Grant for Scientific Schools RSGSS-65751.2010.2.

References

[1] P. A. Bolokhov, M. Shifman, A. Yung, *BPS Spectrum of Supersymmetric* $\mathrm{CP}(N-1)$ *Theory with* Z_N *Twisted Masses,* [arXiv:1104.5241 [hep-th]].

[2] N. Seiberg and E. Witten, *Monopoles, duality and chiral symmetry breaking in* $\mathcal{N} = 2$ *supersymmetric QCD,* Nucl. Phys. B **431**, 484 (1994) [hep-th/9408099];

Electric - magnetic duality, monopole condensation, and confinement in N=2 supersymmetric Yang-Mills theory, Nucl. Phys. B **426**, 19 (1994) [Erratum-ibid. B **430**, 485 (1994)] [hep-th/9407087].

[3] N. Dorey, *The BPS spectra of two-dimensional supersymmetric gauge theories with twisted mass terms,* JHEP **9811**, 005 (1998) [hep-th/9806056].

[4] A. Hanany and D. Tong, *Vortices, instantons and branes,* JHEP **0307**, 037 (2003) [hep-th/0306150].

[5] R. Auzzi, S. Bolognesi, J. Evslin, K. Konishi and A. Yung, *Non-Abelian superconductors: Vortices and confinement in* $\mathcal{N} = 2$ *SQCD,* Nucl. Phys. B **673**, 187 (2003) [hep-th/0307287].

[6] M. Shifman, A. Yung, Phys. Rev. **D70**, 045004 (2004). [hep-th/0403149].

[7] A. Hanany and D. Tong, *Vortex strings and four-dimensional gauge dynamics,* JHEP **0404**, 066 (2004) [hep-th/0403158].

[8] E. B. Bogomol'nyi, *Yad. Fiz.* **24**, 861 (1976) [*Sov. J. Nucl. Phys.* **24**, 449 (1976)], reprinted in *Solitons and Particles*, eds. C. Rebbi and G. Soliani (World Scientific, Singapore, 1984) p. 389; M. K. Prasad and C. M. Sommerfield, *Phys. Rev. Lett.* **35**, 760 (1975), reprinted in *Solitons and Particles*, Eds. C. Rebbi and G. Soliani (World Scientific, Singapore, 1984) p. 530.

[9] A. Gorsky, M. Shifman and A. Yung, *Non-Abelian meissner effect in Yang-Mills theories at weak coupling,* Phys. Rev. D **71**, 045010 (2005) [hep-th/0412082].

[10] M. Shifman, A. Vainshtein and R. Zwicky, *Central charge anomalies in 2D sigma models with twisted mass,* J. Phys. A A **39**, 13005 (2006) [hep-th/0602004].

[11] S. Ölmez and M. Shifman, *Curves of Marginal Stability in Two-Dimensional* $CP(N-1)$ *Models with* Z_N*-Symmetric Twisted Masses,* J. Phys. A A **40**, 11151 (2007) [hep-th/0703149].

[12] M. Kontsevich and Y. Soibelman, *Stability structures, motivic Donaldson-Thomas invariants and cluster transformations*, arXiv:0811.2435 [math.AG].

[13] N. Dorey and K. Petunin, *On the BPS spectrum at the root of the Higgs Branch*,

[14] K. Hori and C. Vafa, *Mirror symmetry,* arXiv:hep-th/0002222.

[15] E. Frenkel and A. Losev, Commun. Math. Phys. **269**, 39 (2006) [arXiv:hep-th/0505131].

[16] M. Shifman, A. Yung, Phys. Rev. **D81**, 085009 (2010). [arXiv:1002.0322 [hep-th]].

[17] N. Dorey, T. J. Hollowood, D. Tong, JHEP **9905**, 006 (1999). [hep-th/9902134].

[18] V.A. Novikov, M.A. Shifman, A.I. Vainshtein, and V.I. Zakharov, *Two-Dimensional Sigma Models: Modeling Nonperturbative Effects of Quantum Chromodynamics,* Phys. Rept. **116**, 103 (1984); A.Y. Morozov, A.M. Perelomov, and M.A. Shifman, Nucl. Phys. **B248**, 279 (1984).

[19] M. Shifman, A. Yung, *Supersymmetric Solitons and How They Help Us Understand Non-Abelian Gauge Theories,* Rev. Mod. Phys. **79**, 1139 (2007). [hep-th/0703267].